

Supporting Information

Kirigami Inspired Island-chain Design for Wearable Perovskite Solar Cells with High Stretchability, Moistureproof Ability and Performance Stability

Jiabin Qi^{ab}, Hao Xiong^b, Chengyi Hou^a, Qinghong Zhang^{b*}, Yaogang Li^b, Hongzhi Wang^{a*}

^aState Key Laboratory for Modification of Chemical Fibers and Polymer Materials, College of Materials Science and Engineering, Donghua University, Shanghai 201620, People's Republic of China

^bEngineering Research Center of Advanced Glasses Manufacturing Technology, MOE, Donghua University, Shanghai 201620, People's Republic of China

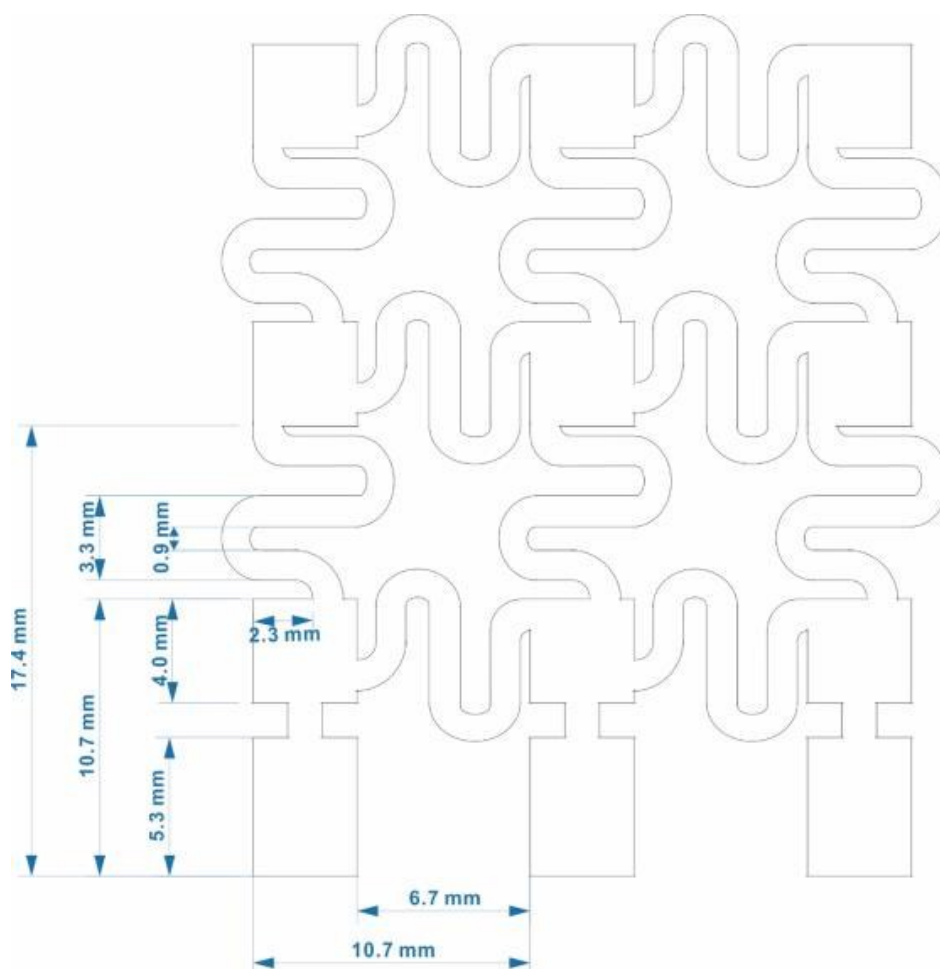


Figure S1. Specific structural parameters of the island-chain design.

* Corresponding author. Tel: +86-21-67792943; fax: +86-21-67792855. E-mail address: wanghz@dhu.edu.cn (H. Z. Wang), zhangqh@dhu.edu.cn (Q. H. Zhang),

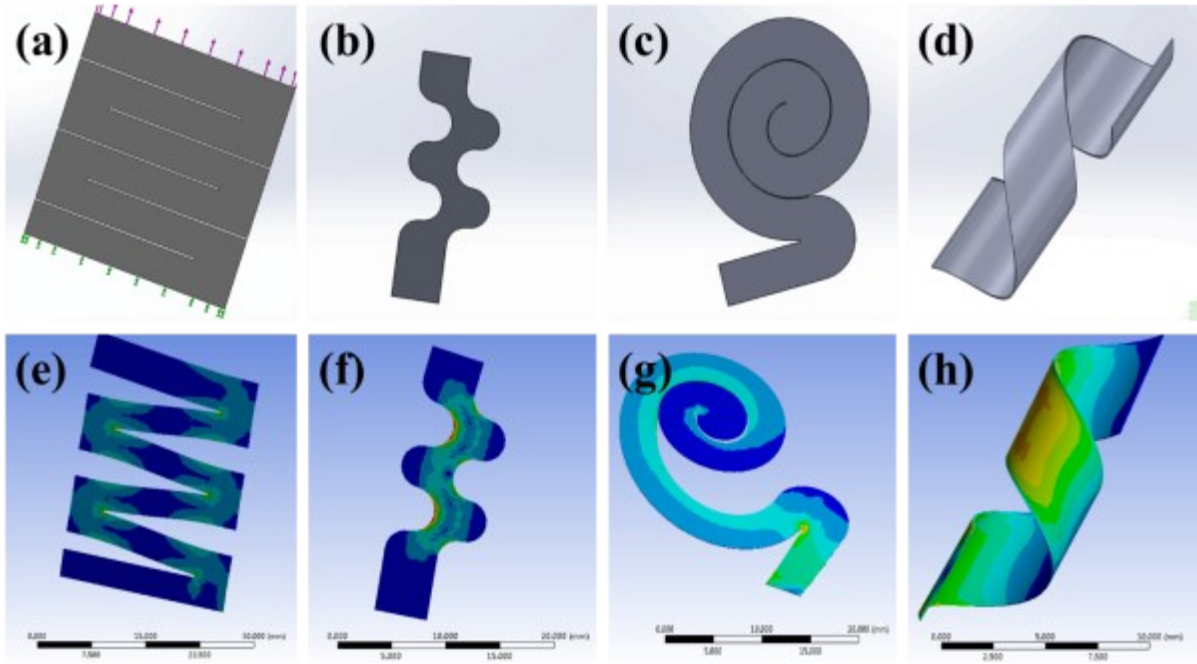


Figure S2. Illustrations and finite element analysis patterns of designed structures.

As shown by the yellow area, stress concentrated at the turning point, where it is easy to tear the PSC, making it unusable.

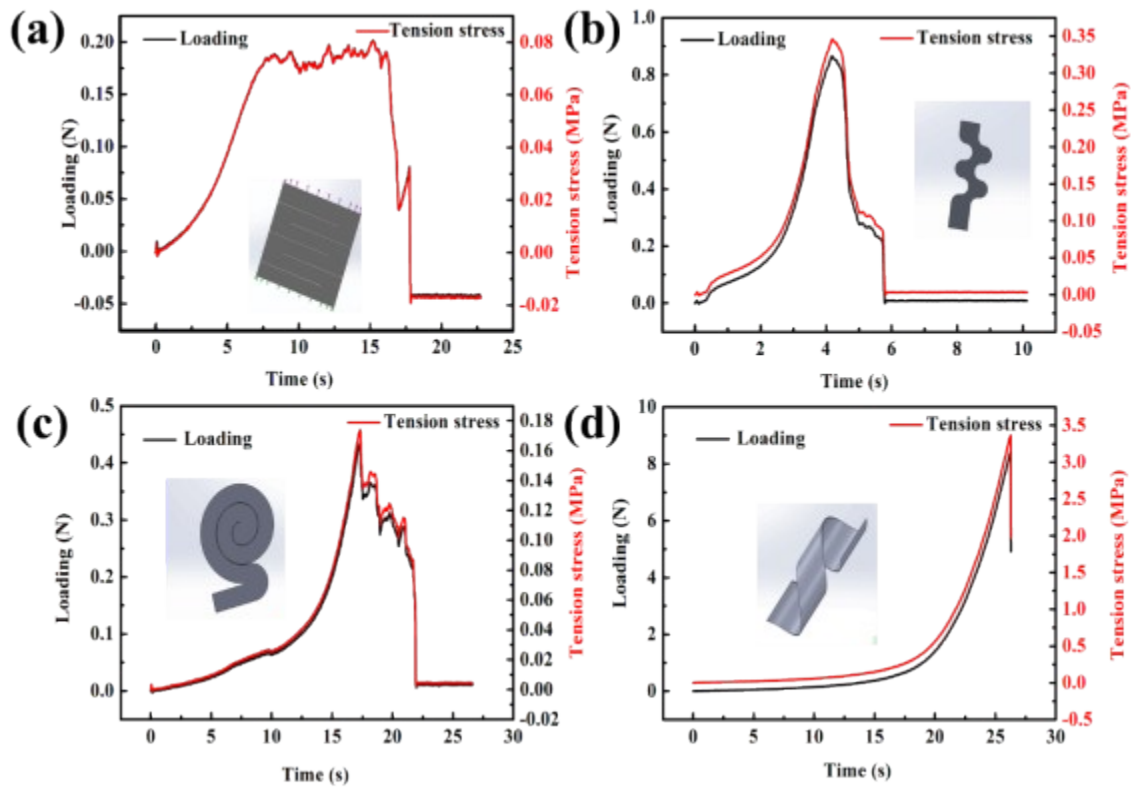


Figure S3. Diagrams of mechanical properties related to the designed stretchable structures.

The stress and strain of the first three structures were minimal. Loading was less than 1 N, and the tensile stress was less than 0.5 MPa. However, the fourth structure was unlike the first three. The stress and strain were considerable; however, it was difficult to break the device, mainly owing to the contraction of the space during the tensile process.

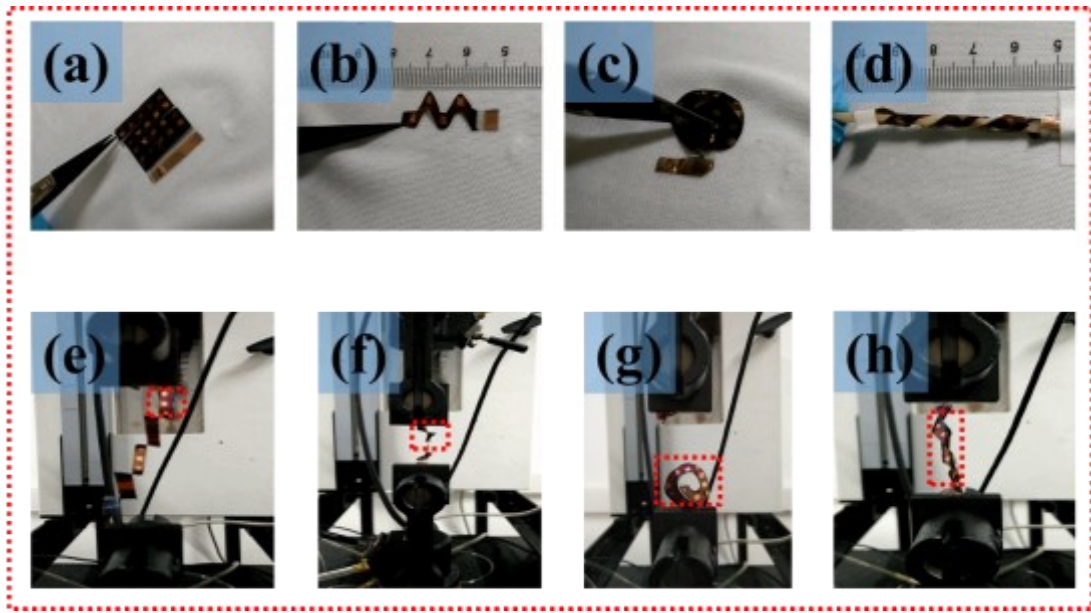


Figure S4. Photographs showing the state of device during test with omnipotent material machine.

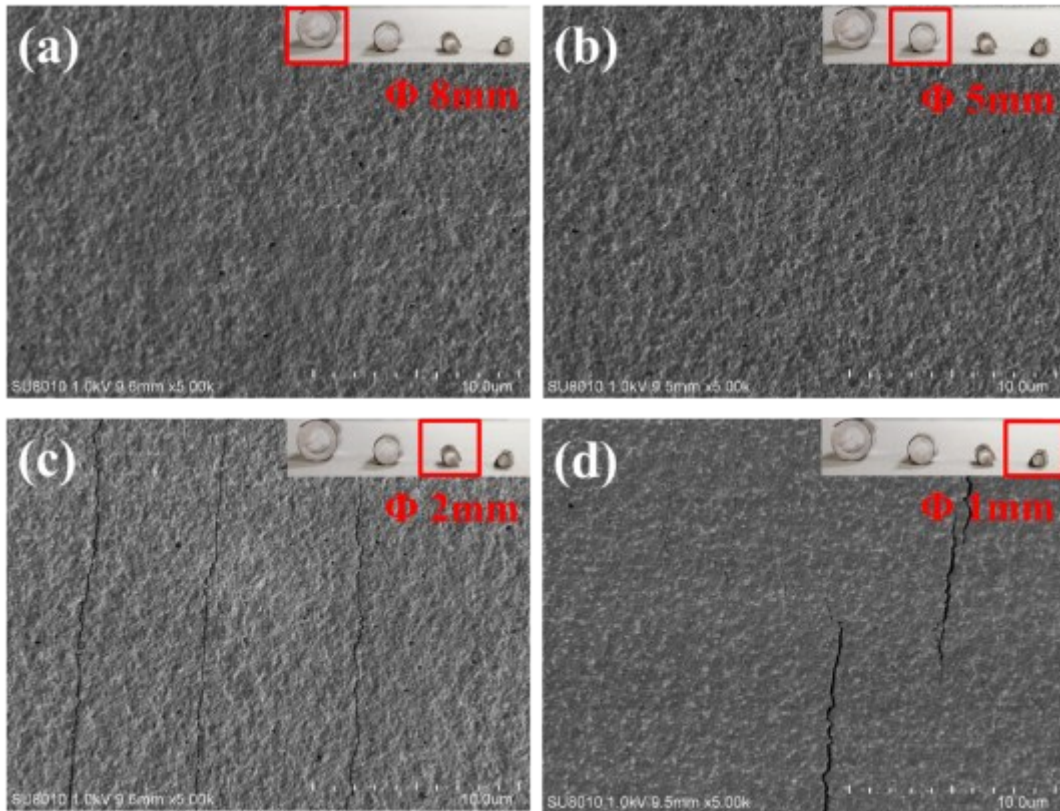


Figure S5. Magnified SEM image of regions subjected to different strains.

Severe bending generated cracks, which degraded the device performance. The bending strain caused by stretching can be divided into two types of behavior: a low strain region ($r \geq 2$ mm) and high strain region ($r < 2$ mm). There was no cracking in the low-strain region; however, multiple cracks were observed in the high-strain region (**Figure S5d**)

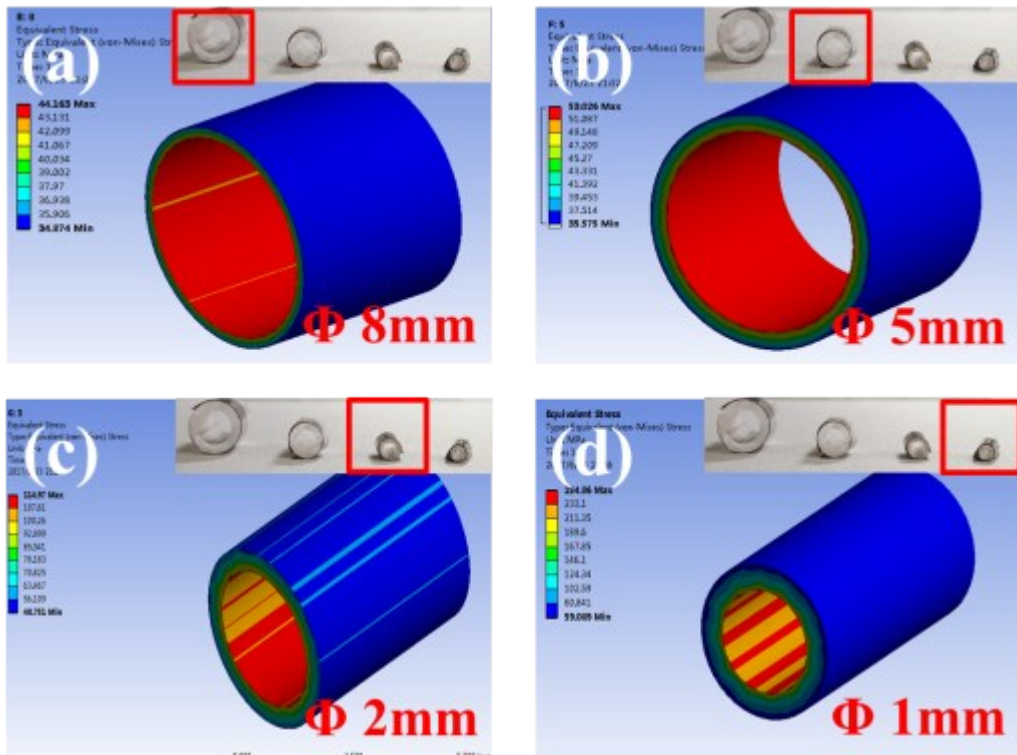


Figure S6. Finite element analysis patterns of regions subjected to different strains.

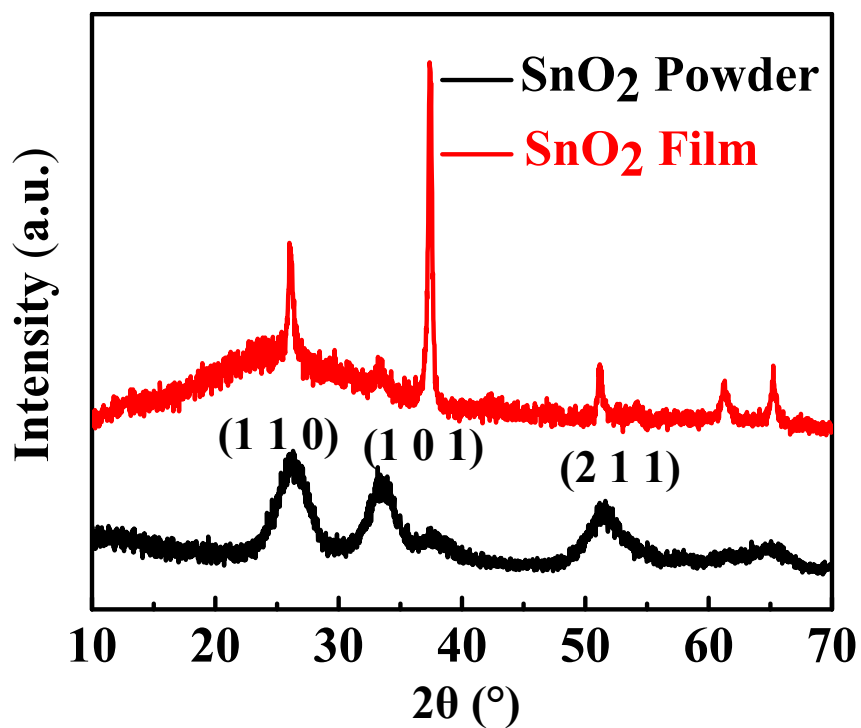


Figure S7. XRD patterns of the low-temperature synthesized SnO₂ powders and spin-coated thin films.

All peaks were consistent with a tetragonal SnO₂ structure (space group P42/mnm, $a=0.4738$ nm and $c=0.3187$ nm). No peaks of the starting substance or any residual species were found in the XRD pattern, indicating the synthesis of pure SnO₂ crystals

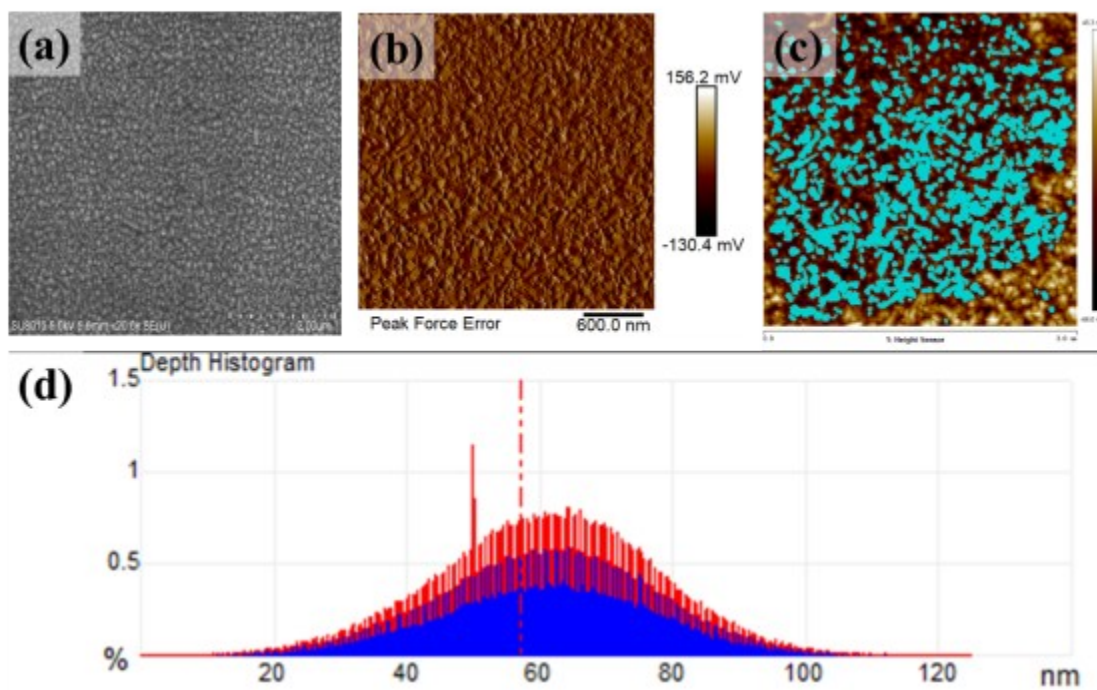


Figure S8. Surface morphology of the SnO₂ thin film studied by SEM (a) and top-view atomic force microscopy (b, c); size distribution of SnO₂ crystals (d).

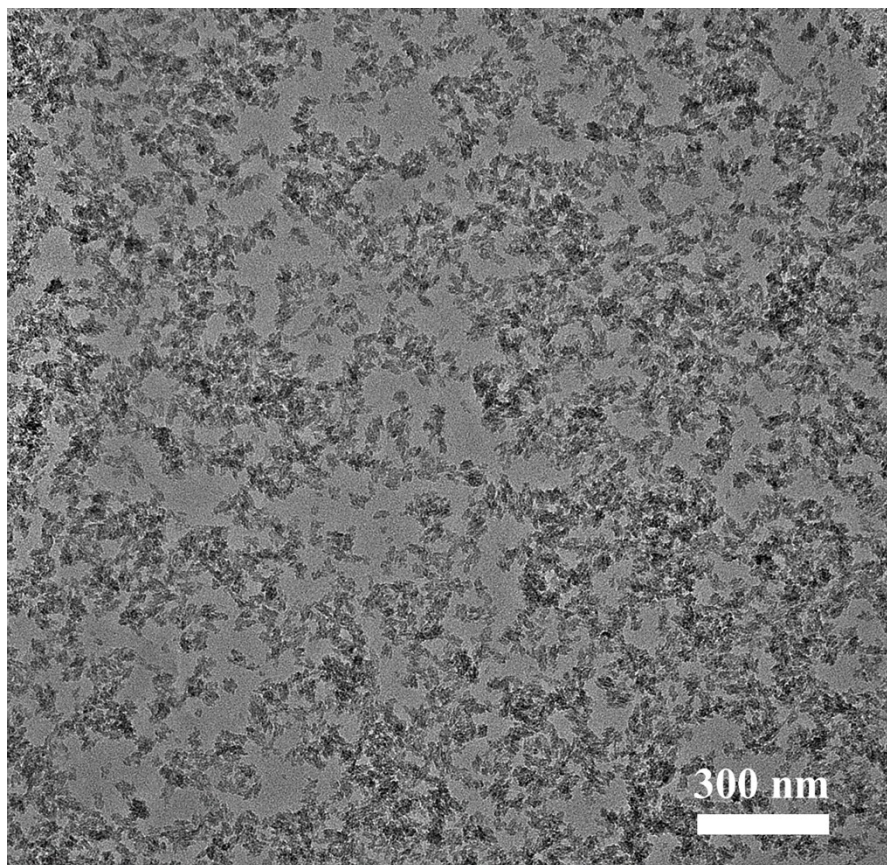


Figure S9. Bright-field TEM image of hydrothermal SnO₂ nanocrystals.

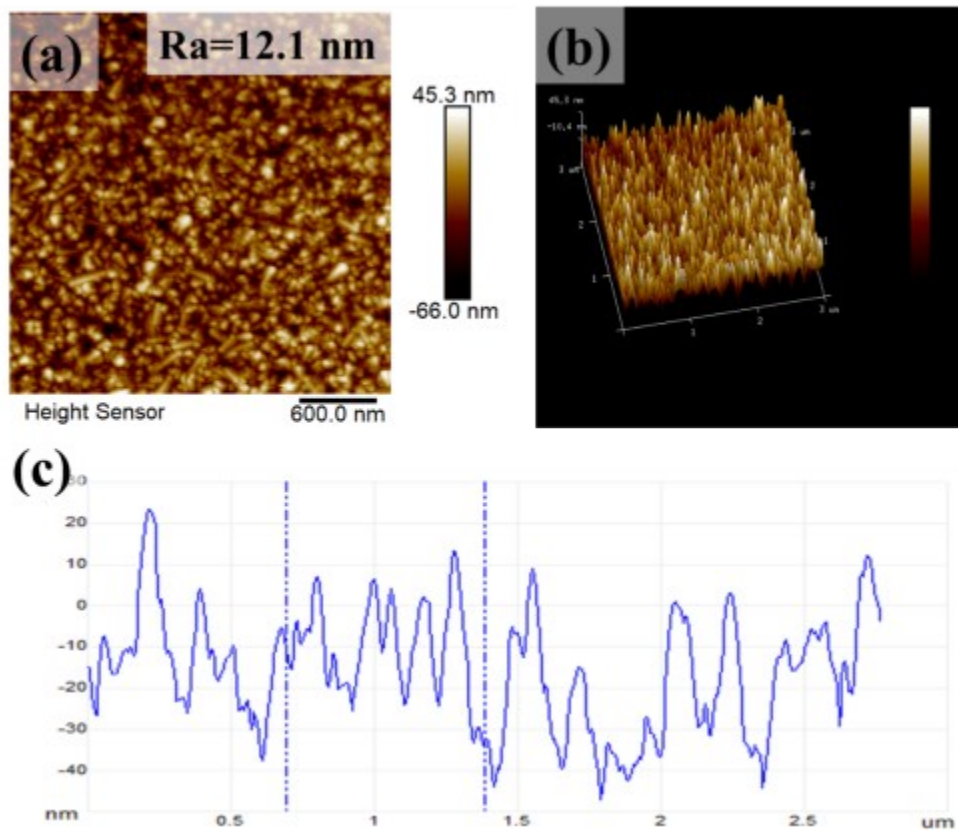


Figure S10. AFM images of the SnO₂ films with a root-mean-square roughness of 12.1 nm.

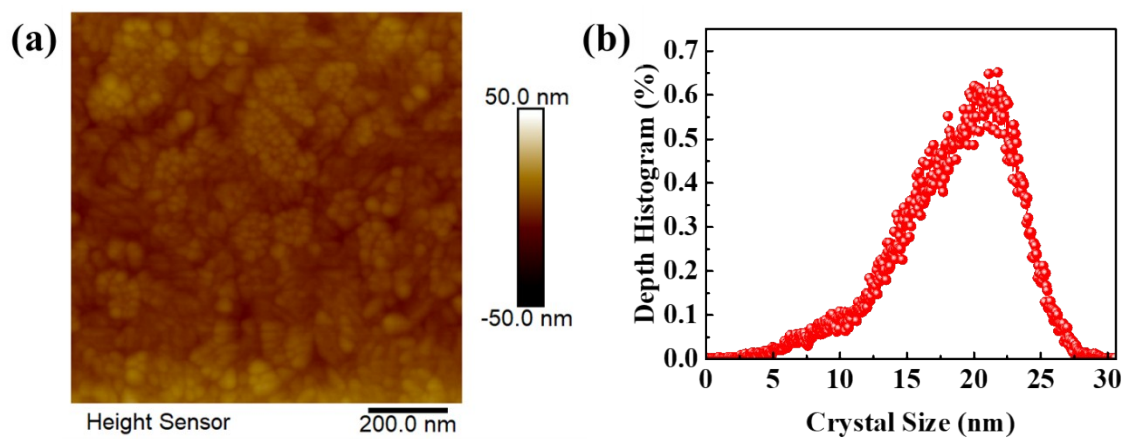


Figure S11. Top-view atomic force microscopy (a) and size distribution (b) of ITO crystals.

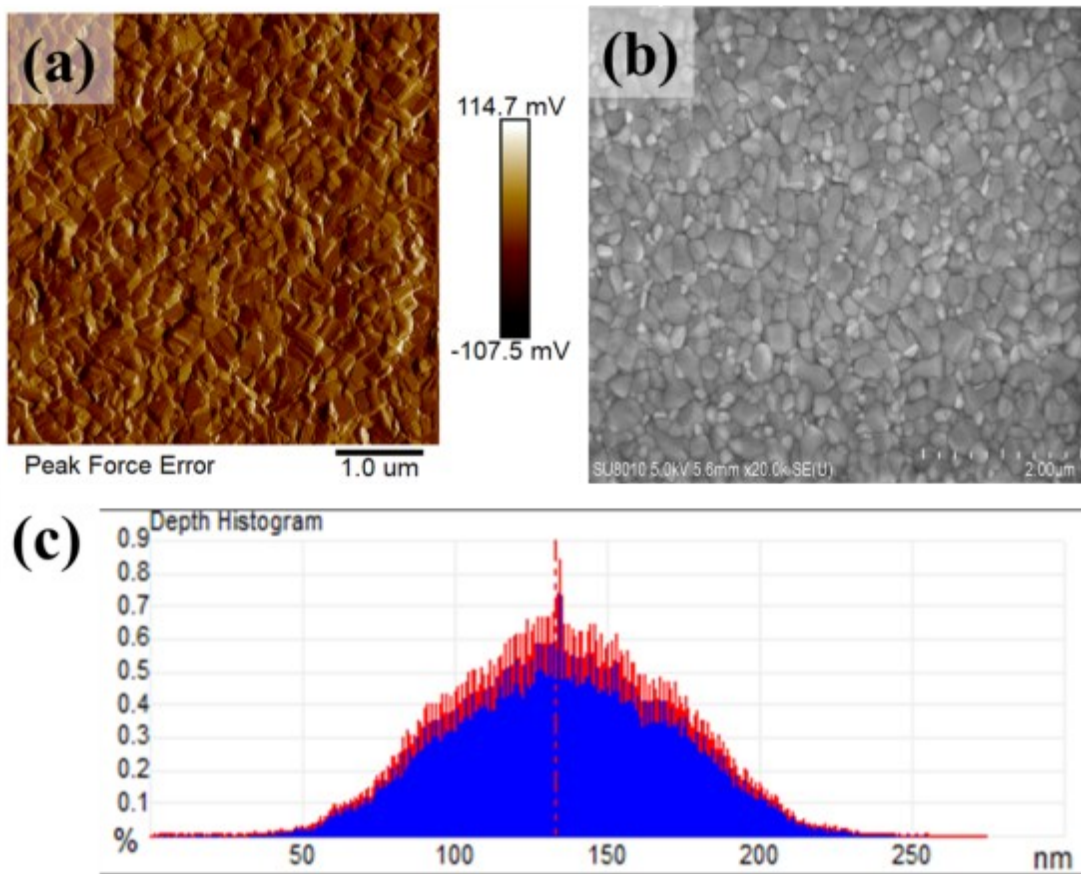


Figure S12. Surface morphology of perovskite film studied by top-view atomic force microscopy (a) and SEM (b); size distribution of perovskite crystals (c).

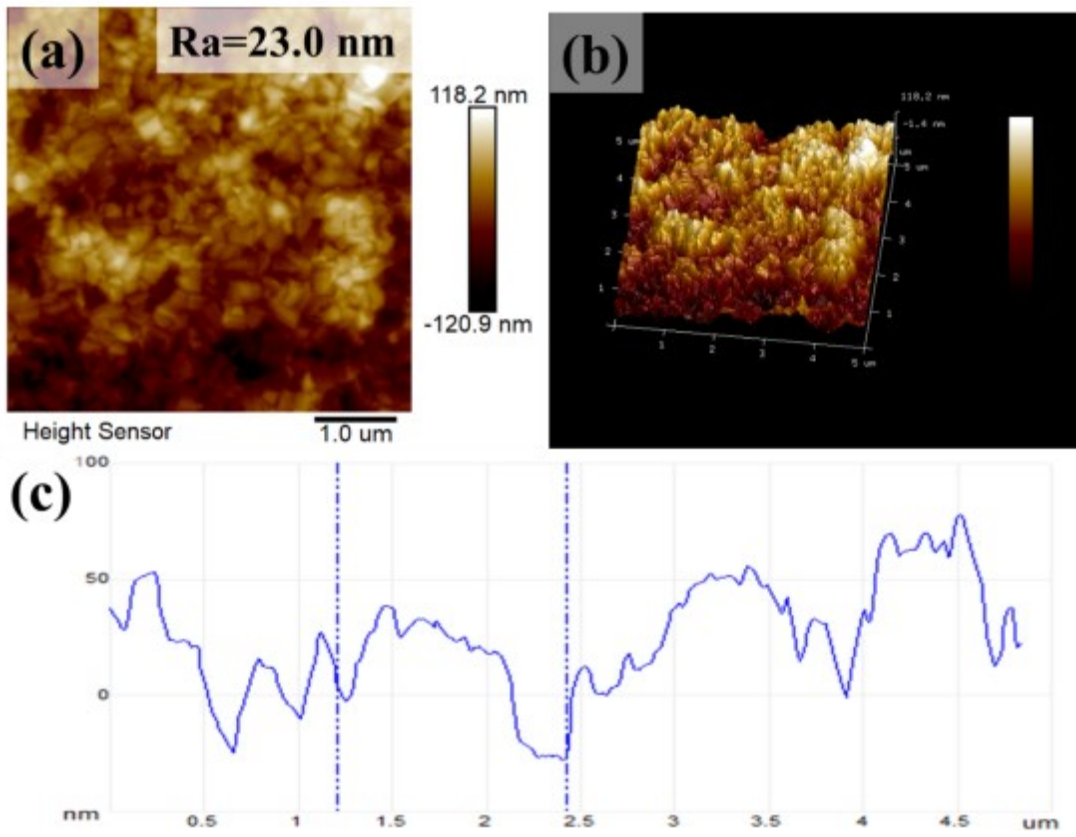


Figure S13. AFM height images of the perovskite films with root-mean-square roughness 23.0 nm.

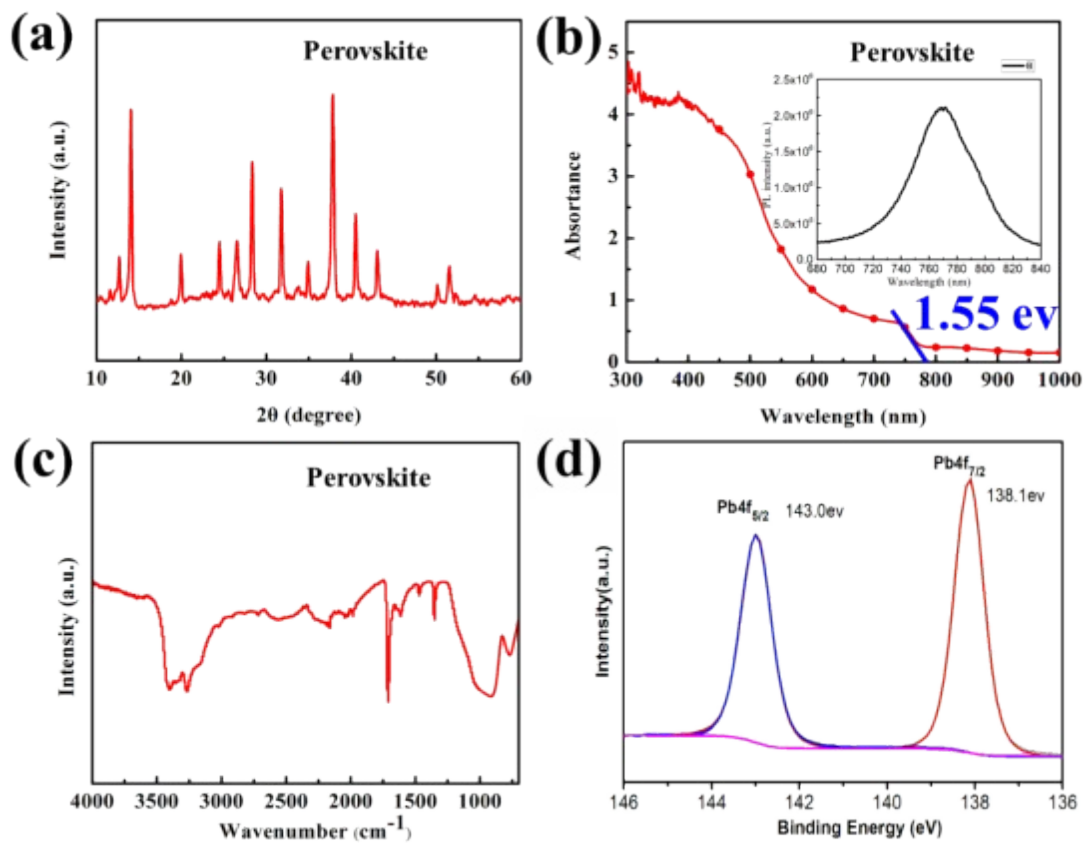


Figure S14. XRD pattern (a), absorbance spectra with insets showing steady-state photoluminescence spectra (b), Fourier transform infrared spectroscopy (FTIR) spectra (c), and typical X-ray photoelectron spectroscopy (XPS) survey scan (d) of the perovskite film.

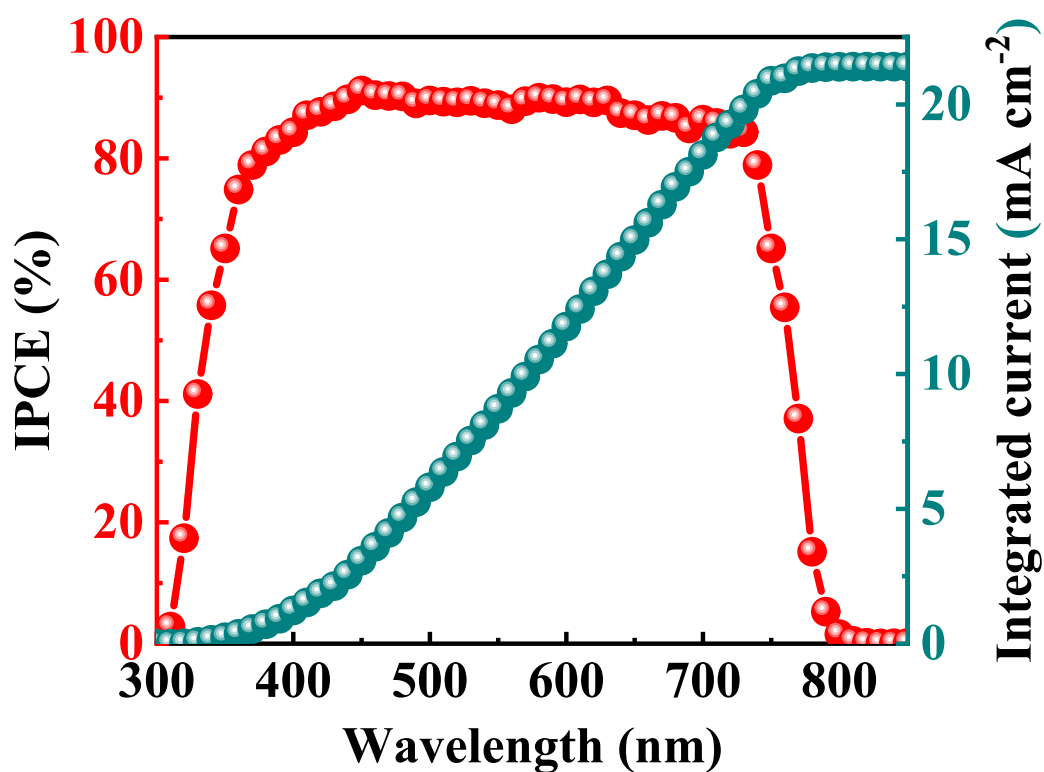


Figure S15. Representative external quantum efficiency of the PSC device.

A sharp increase in the wavelength of the IPCE curve is consistent with the absorption edge data, which appeared at approximately 780 nm. In the visible region, the external quantum efficiency reached up to 90%. The integrated short-circuit current (22.4 mA cm^{-2}) matched well with the J-V results. The high short-circuit current can be attributed to the high quality of the uniform perovskite film.

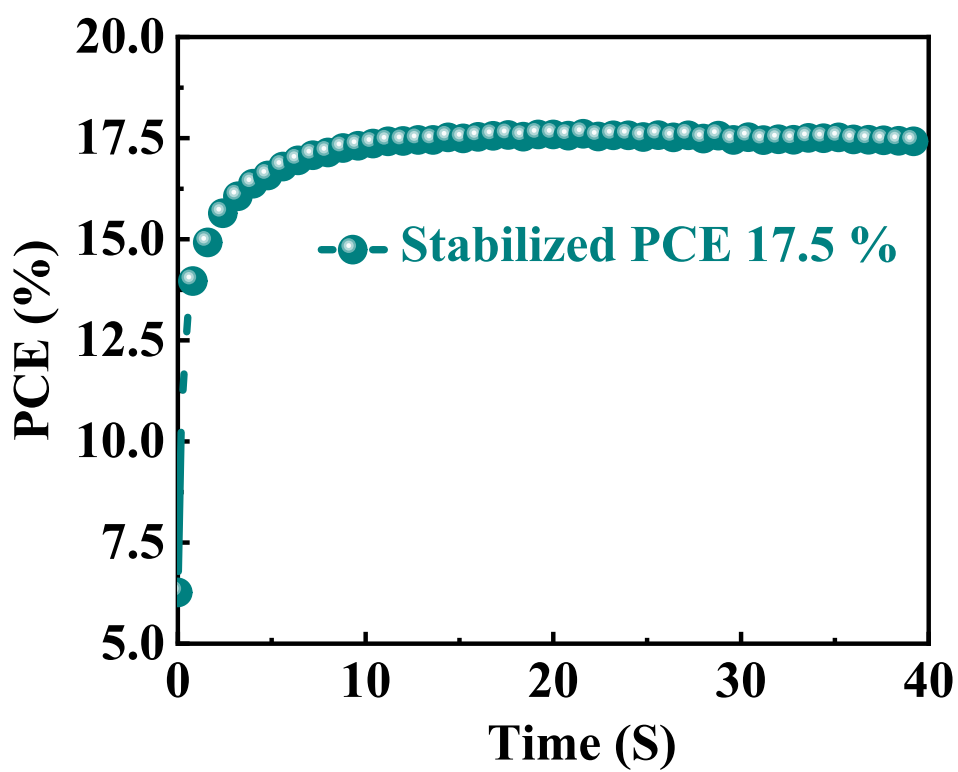


Figure S16. Stable output of power conversion efficiency as a factor of time.

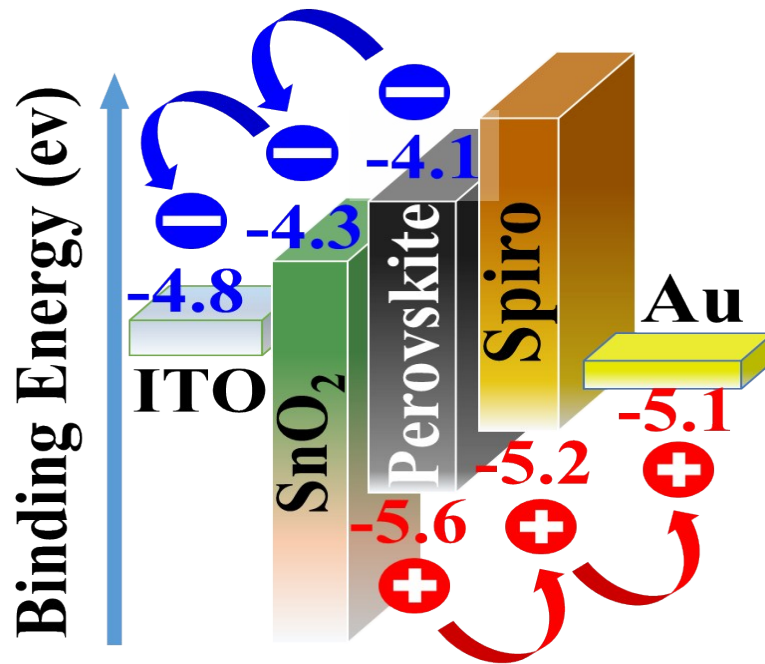


Figure S17. Energy diagram of the structure of the PSC device.

The energy diagram of the device structure indicates sufficient energy deviation in a single layer can cause holes and electrons to move towards the corresponding electrodes. The work function (WS), valence band maximum (VBM) and bandgap (E_g) of the SnO₂ nanocrystals are 4.36, 3.74, and 3.79 eV, respectively.[1] The conduction band (EC) of the SnO₂ nanocrystals was calculated from the band structure of the semiconductor to be 4.31 eV, as determined from $EC = WS + VBM - E_g$. In principle, a deeper conduction band and the high mobility of SnO₂ promotes charge transfer from the perovskite to the electron transport layer, indicating a reduced energy barrier. These features suggest that SnO₂-based PSCs can provide good stable performance.

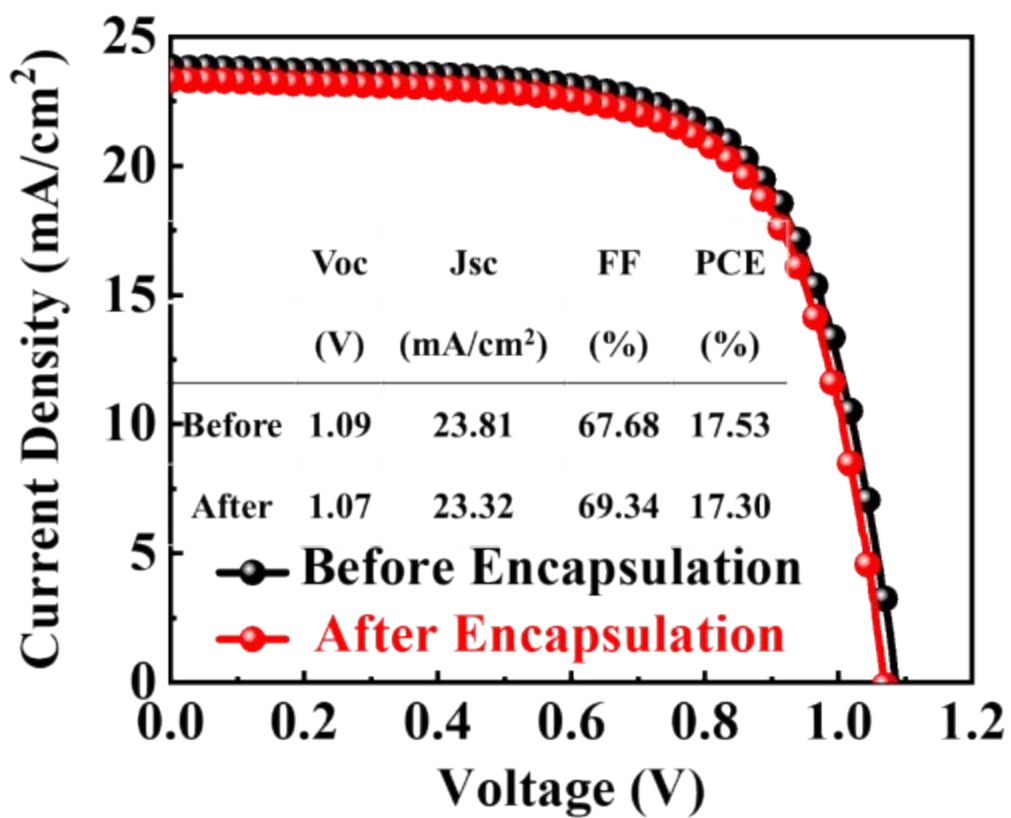


Figure S18. Output performance of perovskite solar cells before and after covering with Eco-flex film.

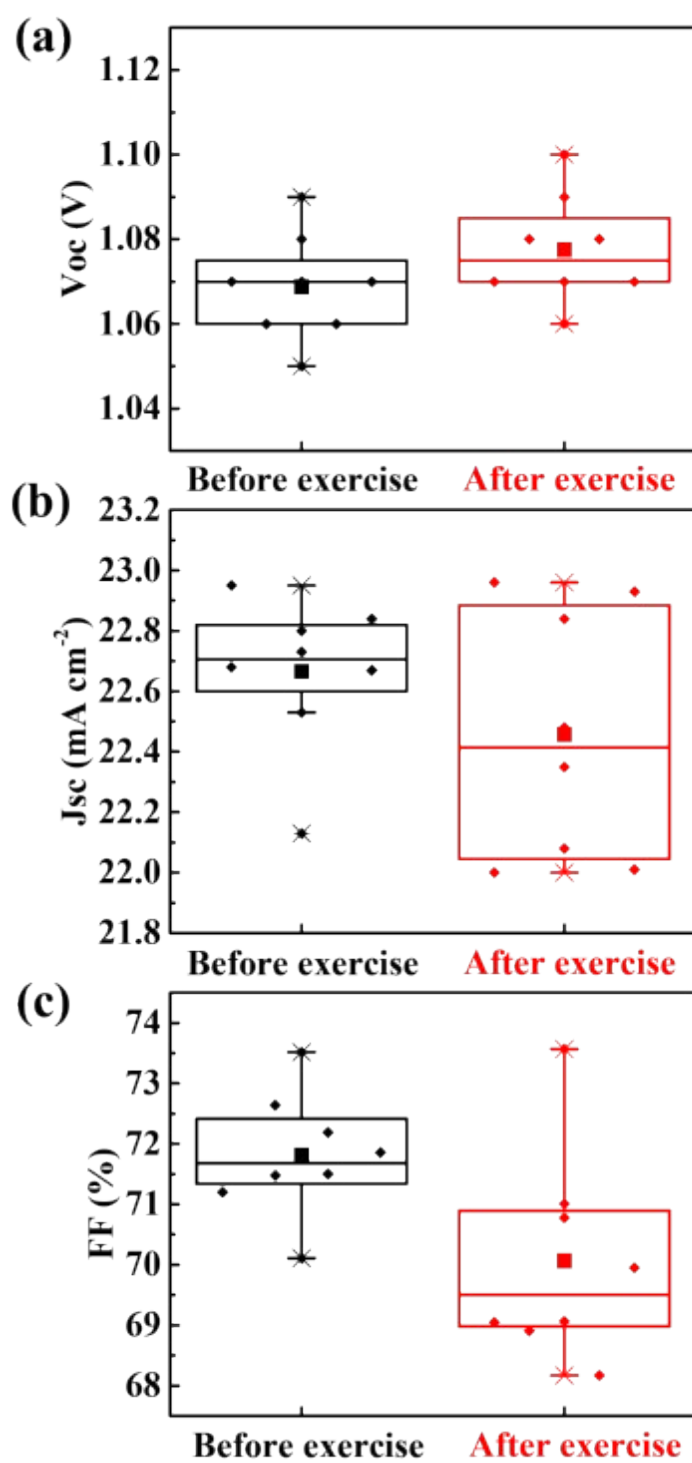


Figure S19. V_{oc} , J_{sc} , and FF statistics of eight devices measured before and after exercise.

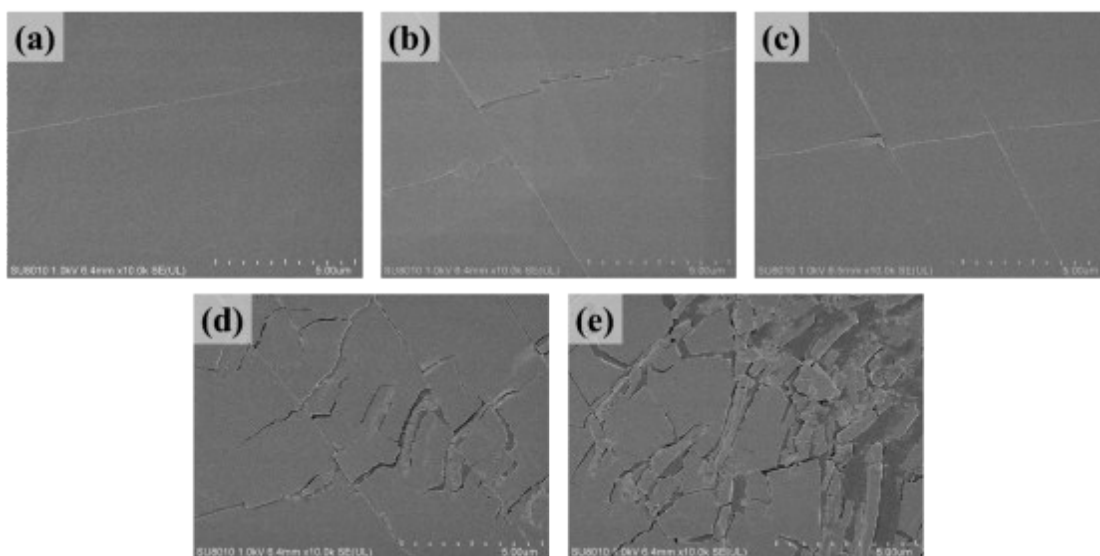


Figure S20. SEM photos of cracks in ITO film at strain of (a) 0%, (b) 50%, (c) 80%, (d) 110%, and (e) 140%

Table S1. Key J-V parameters of PSCs covered with Eco-flex film after soaking in water for different periods of time.

	Voc	Jsc	FF	PCE
	(V)	(mA/cm²)	(%)	(%)
0 s	1.08	22.85	68.17	16.87
30 s	0.86	20.27	63.16	11.05
60 s	0.74	10.80	32.64	2.63
90 s	0.10	6.63	27.76	0.19

Table S2. Key J-V parameters of PSCs during stretching process of different strain ratio.

	Voc	Jsc	FF	PCE
	(V)	(mA/cm²)	(%)	(%)
0%	1.096	22.41	71.97	17.68
50%	1.083	23.02	69.11	17.24
80%	1.085	22.59	68.09	16.70
110%	1.072	21.36	57.64	13.21
140%	0.929	11.75	48.03	5.25

References

- (1) Q. Jiang, L. Zhang, H. Wang, X. Yang, J. Meng, H. Liu, Z. Yin, X. Zhang, J. You, Enhanced electron extraction using SnO₂ for high-efficiency planar-structure HC(NH₂)₂PbI₃-based perovskite solar cells, Nat. Energy 2 (2016) 16177.